



# **AE (Acoustic Emission) for Flip-Chip CGA/FCBGA Defect Detection**

Reza Ghaffarian, Ph.D.  
Jet Propulsion Laboratory  
Pasadena, California

Jet Propulsion Laboratory  
California Institute of Technology  
Pasadena, California

JPL Publication 14-12 4/17



# **AE (Acoustic Emission) for Flip-Chip CGA/FCBGA Defect Detection**

NASA Electronic Parts and Packaging (NEPP) Program  
Office of Safety and Mission Assurance

Reza Ghaffarian, Ph.D.  
Jet Propulsion Laboratory  
Pasadena, California

NASA WBS: 724297.40.43  
JPL Project Number: 104593  
Task Number: 40.49.02.15

Jet Propulsion Laboratory  
4800 Oak Grove Drive  
Pasadena, CA 91109

<http://nepp.nasa.gov>

This research was carried out at the Jet Propulsion Laboratory, California Institute of Technology, and was sponsored by the National Aeronautics and Space Administration Electronic Parts and Packaging (NEPP) Program.

Reference herein to any specific commercial product, process, or service by trade name, trademark, manufacturer, or otherwise, does not constitute or imply its endorsement by the United States Government or the Jet Propulsion Laboratory, California Institute of Technology.

©2014. California Institute of Technology. Government sponsorship acknowledged.

### Acknowledgments

The author would like to acknowledge many people from industry, especially Ken Tylor, and the Jet Propulsion Laboratory (JPL), especially Steve Bolin, who were critical to the progress of this activity. The author extends his appreciation to program managers of the National Aeronautics and Space Administration Electronics Parts and Packaging (NEPP) Program, including Michael Sampson, Ken LaBel, Dr. Charles Barnes, and Dr. Douglas Sheldon, for their continuous support and encouragement.

## OBJECTIVES AND PRODUCTS

Flip-chip (FC) die is the only known technique that enables high I/O (>1000) ball grid array/column grid array (BGA/CGA) electronic packages. One of the key drawbacks of packages with solder balls/columns and solder joint interconnections under the flip-chip die is that inspection for workmanship defects can be challenging—whether using nondestructive evaluation (NDE) by X-ray or acoustic microimaging (AMI) approaches. Particularly, acoustic microimaging inspection becomes even more difficult because of interference from other materials, especially when packages are assembled onto PCB. The applicability of AMI for defect detection of assemblies, especially its C-mode scanning acoustic microscopy (C-SAM), was explored.

This report presents the NDE and C-SAM approaches through transmission evaluation results. Images of through thickness layers by C-SAM along with their representative images by 2D X-ray are presented for a number of advanced electronics package assemblies, especially FCBGA and FC-CGA. Key features, detectable by a C-SAM system, show the advantages and limitations of this NDE inspection tool, especially when used for packages assembled onto PCB. The C-SAM has the added capability of detecting features (such as delamination) that an X-ray system lacks adequate contrast for. Microelectronic samples to be evaluated by C-SAM should be resistant to liquid exposure, whereas those to be evaluated by X-ray should be resilient to radiation bombardment.

**Key words:** Acoustic microscopy, AE, AMI, C-SAM, FCBGA, FC-CGA, real time X-ray, 2D X-ray, Column grid array, CGA

## TABLE OF CONTENTS

1.0	EXECUTIVE SUMMARY .....	5
2.0	Acoustic Emission Technology .....	7
2.1	Electronic Packaging Trend .....	7
2.2	Inspection Challenges .....	8
2.3	Acoustic Microimaging and C-SAM .....	8
2.4	AMI for Plastic Encapsulated Microcircuits (PEM) Evaluation .....	10
2.5	C-SAM of Flip-Chip and Underfill .....	11
3.0	Experimental Evaluation by C-SAM .....	14
3.1	Test Plan and Evaluation Approaches .....	14
3.2	Plastic LGA132 .....	14
3.3	Flip-Chip BGA1704 with Heat Sink .....	16
3.4	Flip-Chip CGA1752 with Heat Sink .....	16
3.5	Flip-Chip LGA1517/CGA without Heat Sink .....	17
3.6	Fine Pitch PBGAs 432 and 676 I/O .....	19
3.7	C-SAM Repeat of CGA1752 after Heat Sink Removal .....	20
3.8	Hermetically Sealed CGA1272 with Internal Wire Bonds .....	20
3.9	Plastic LGA 1156 I/O and Fine Pitch Package Assemblies .....	21
3.10	Effect of 20 Solder Iron Touches at 700°F .....	21
3.11	Cross-sectional Characterization of LGA1517 .....	22
4.0	Conclusions .....	23
5.0	References .....	25
6.0	ACRONYMS AND ABBREVIATIONS .....	26

## 1.0 EXECUTIVE SUMMARY

C-mode scanning acoustic microscopy (C-SAM) is a nondestructive inspection technique that uses ultrasound to show the internal feature of a specimen. A very high or ultra-high-frequency ultrasound passes through a specimen to produce a visible acoustic microimage (AMI) of its inner features. As ultrasound travels into a specimen, the wave is absorbed, scattered or reflected. The response is highly sensitive to the elastic properties of the materials and is especially sensitive to air gaps. This specific characteristic makes AMI the preferred method for finding “air gaps” such as delamination, cracks, voids, and porosity. C-SAM analysis, which is a type of AMI, was widely used in the past for evaluation of plastic microelectronic circuits, especially for detecting delamination of direct die bonding. With the introduction of the flip-chip die attachment in a package; its use has been expanded to nondestructive characterization of the flip-chip solder bumps and underfill.

Figure 1.1 compares visual and C-SAM inspection approaches for defect detection, especially for solder joint interconnections and hidden defects. C-SAM is specifically useful for package features like internal cracks and delamination. C-SAM not only allows for the visualization of the interior features, it has the ability to produce images on layer-by-layer basis. Visual inspection; however, is only superior to C-SAM for the exposed features including solder dewetting, microcracks, and contamination. Ideally, a combination of various inspection techniques—visual, optical and SEM microscopy, C-SAM, and X-ray— need to be performed in order to assure quality at part, package, and system levels.

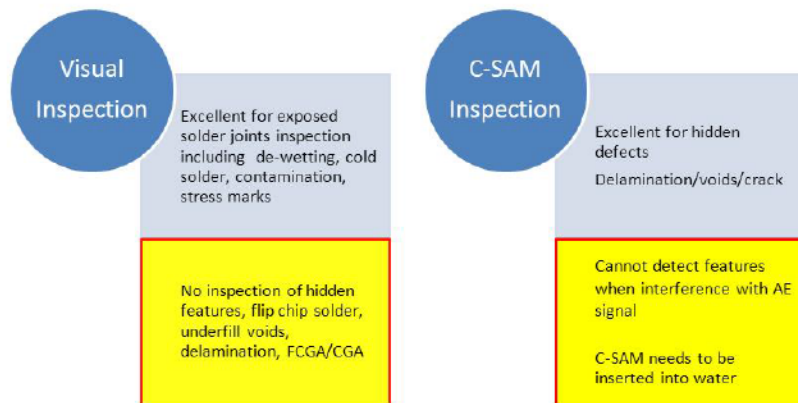


**Figure 1-1.** Strengths and weaknesses of using C-SAM vs. visual inspection to detect key package defects.

This reports presents evaluations performed on various advanced packages/assemblies, especially the flip-chip die version of ball grid array/column grid array (BGA/CGA) using C-SAM equipment. Both external and internal equipment was used for evaluation. The outside facility provided images of the key features that could be detected using the most advanced C-SAM equipment with a skilled operator. Investigation continued using in-house equipment with its limitations. For comparison, representative X-rays of the assemblies were also gathered to show key defect detection features of these non-destructive techniques. Key images gathered and compared are:

- Compared the images of 2D X-ray and C-SAM for a plastic LGA assembly showing features that could be detected by either NDE technique. For this specific case, X-ray was a clear winner.
- Evaluated flip-chip CGA and FCBGA assemblies with and without heat sink by C-SAM. Only the FC-CGA package that had no heat sink could be fully analyzed for underfill and bump quality. Cross-sectional microscopy did not revealed peripheral delamination features detected by C-SAM.
- Analyzed a number of fine pitch PBGA assemblies by C-SAM. Even though the internal features of the package assemblies could be detected, C-SAM was unable to detect solder joint failure at either the package or board level.

- Twenty times touch ups by solder iron with 700°F tip temperature, each with about 5 second duration, did not induce defects to be detected by C-SAM images. Other techniques need to be considered to induce known defects for characterization.

Given NASA's emphasis on the use of microelectronic packages and assemblies and quality assurance on workmanship defect detection, understanding key features of various inspection systems that detect defects in the early stages of package and assembly is critical to developing approaches that will minimize future failures. Additional specific, tailored non-destructive inspection approaches could enable low-risk insertion of these advanced electronic packages having hidden and fine features.

## 2.0 ACOUSTIC EMISSION TECHNOLOGY

### 2.1 Electronic Packaging Trend

Previous generations of microelectronic packaging technology aimed mostly at meeting the needs of high-reliability applications, such as the ceramic leaded quad flat package (CQFP). Nondestructive wire bond pull at the package level and subsequent visual inspection for solder joint integrity at the board level were adequate for ensuring the quality of CQFPs. Consumer electronics are now driving miniaturization trends for electronic packaging and assembly; they introduce a vast number of area array packages. The array packages initially only had hidden solder joints under the bottom area of the package; now the flip-chip die within package also have hidden joints. The hidden joints—both at package and assembly levels—added significant challenges to the inspectability and certainty of assuring integrity at the various microelectronics hierarchy levels. Another added complexity is the transition to using only Pb-free solder alloys. Suppliers of electronics packages either have or will soon transition to using Pb-free alloys in order to enforce restrictions on hazardous substances (ROHS) for electronic systems. The solder joint appearance for the Pb-free solder alloys is dull rather than shiny, as it is for the tin-lead eutectic solder, which will add confusion even if visual inspection is used inadvertently as a criterion for the quality of joint acceptance or rejection.

Until recently, high-reliability applications have successfully utilized ceramic versions of plastic packages, such as the plastic ball-grid-array (PBGA) or its analogous ceramic ball-grid-array and column-grid-array (CBGA and CGA). Today, there are fewer ceramic versions and they are generally lagging in technology compared to plastic ones [1-5]. Inspection of CGA is challenging. Nondestructive X-ray inspection became a new approach for ensuring the quality of area array packages and assemblies. Even though X-ray can detect the level of voids and bridges of solder joints hidden under packages, it become of less value for detecting solder attachment and underfill integrity of higher I/O (>1000 I/Os) packages with flip-chip die technology (such as FCBGA and FC-CGA; see Figure 2.1). Ceramic substrates considered for high-reliability applications are heavier and less penetrable to X-ray radiation than plastic, making them even more difficult to inspect for this category of packages and assemblies.

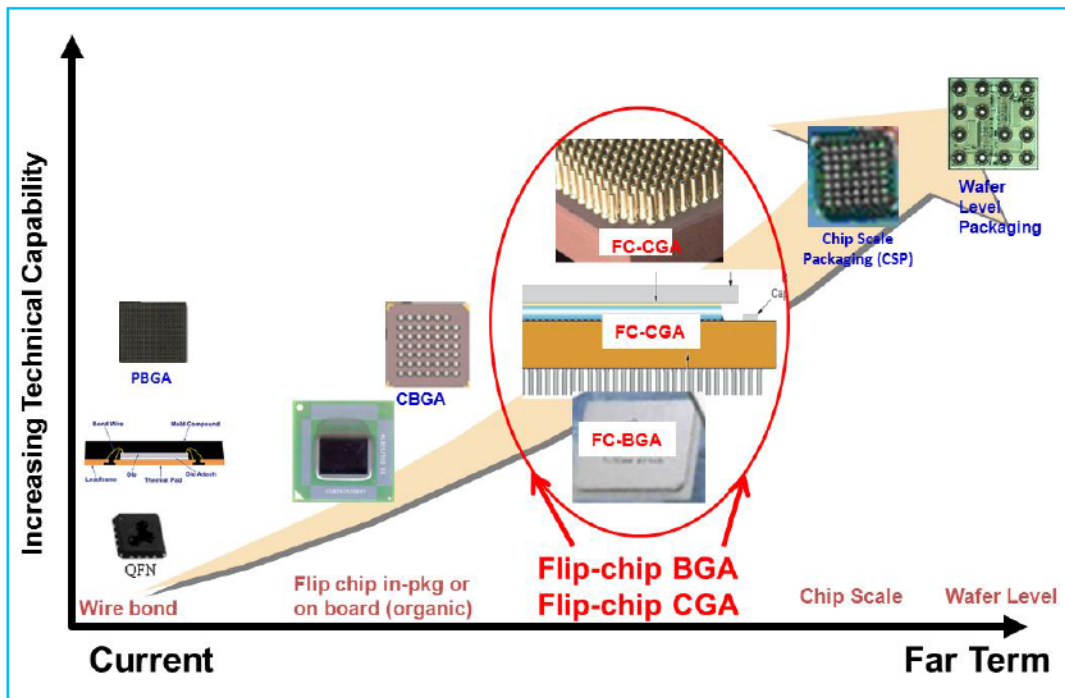


Figure 2-1. Microelectronic trends for single packaging technologies including flip-chip BGA and CGA.

## 2.2 Inspection Challenges

For high-reliability electronic applications, quality assurance personnel are traditionally responsible to perform visual inspection at various package and assembly build steps. For example, at assembly level, solder joints are inspected and either accepted or rejected based on specific sets of workmanship requirements. Further assurance of electronic subsystems or systems is gained by subsequent short-time environmental exposures, including thermal cycles, vibration, and mechanical shock testing. These screening tests also allow for assessing the progress of workmanship anomalies and failures due to workmanship defects or design flaws at either subsystem or system levels. For standard packages, visual inspection alone is generally performed at the package stage, prior to its sealing (pre-cap), as well as at several steps during assembly and at subsystem levels.

Even with the advancements in optical microscopy, while very effective for inspection of standard electronics; visual inspections have limited usefulness for extremely small, dense electronics, especially for flip-chip die with underfill. Such inspection provides some usefulness, but only for the periphery of solder balls of area array packages with large balls and high stand off; it has no value for hidden ball/column arrays under the package; irrespective of stand-off height. Scanning electron microscope SEM and other advanced magnification tools may be used to inspect miniature packages, but generally are not suitable for assembly and systems levels because of the SEM equipment size limitations and hardware handling issues. Even for a single small package, damage due to handling and electrostatic discharge (ESD) is of critical importance. These issues limit the wider use of SEM and other advanced evaluation techniques for active packages with ESD sensitivity.

The inspection system's ability to identify, measure, and analyze defect data after assembly is also critical. Inspection of the solder joint integrity of BGAs/CGAs is important, but cannot be effectively performed by visual inspection. Inspection of fine internal structures of microelectronics assemblies and the alignment of hidden microcircuit interconnect structures, bridges, and voids in BGA/CGA assemblies, may be carried out using real-time X-ray techniques. X-ray also has limitations; it is unable to detect the package internal delamination for either standard die attachent or flip-chip die with underfill, for example. Underfill does not provide sufficient contrast in X-ray imaging to analyze its condition. Non-destructive techniques using acoustic microscopy, especially C-SAM, are needed for such evaluation. This technique, discussed further in the following sections, was used for defect detection of packages and assemblies.

C-SAM inspection of solder joints to the board, particularly for PBGAs and FCBGA/CGA, is also of great importance and should be pursued. However, knowing the role of dissimilar materials and their interface effect on C-SAM signals, access to the substrate solder balls/column level is difficult, if not impossible, through the PCB side of the assembly. The composite board material tends to be extremely attenuating to the ultrasound. Basically, the more composite and copper layers are present, the greater the attenuation. Also, vias in the boards located in the proximity of the solder joints causes excessive scattering of the signal, which interferes with the data. For these reasons, to access the second level solder joint, the C-SAM was performed through the device itself, providing no other defects exist in the device that could block the ultrasonic signal from that level. C-SAM images from these evaluations also presented.

## 2.3 Acoustic Microimaging and C-SAM

Acoustic microscopes emit ultrasounds ranging from 5 MHz to more than 400 MHz, so that micrometer size resolution can be achieved [6]. Ultrasound that penetrates a sample may be scattered, absorbed or reflected by the internal features of the material itself. These actions are analogous to the behavior of light. Ultrasound that is reflected from an internal feature has traveled through the entire thickness of the sample, and is used to make acoustic images. Figure 2.2 schematically compares a few features of flip chip CGA/BGA detectable by AMI and X-ray. X-ray uses high-energy electromagnetic radiation with shorter wavelengths than ultraviolet light to detect inner features. They are highly penetrable depending on the X-ray's energy, which increases with frequency. As frequency and thus penetration increase, the type of X-ray moves from "soft" to "hard." The reflective nature of AMI allows for detection of delamination, whereas the penetration of X-ray allows detection of both short and large voids. These two inspection approaches are complementary techniques that should be used to reveal different features. The X-ray technique relies on the differential attenuation of X-ray energy, whereas the AMI technique relies on material change. The practical result is that AMI is orders of magnitude more sensitive for detecting air space type defects such as voids, delaminations and cracks.

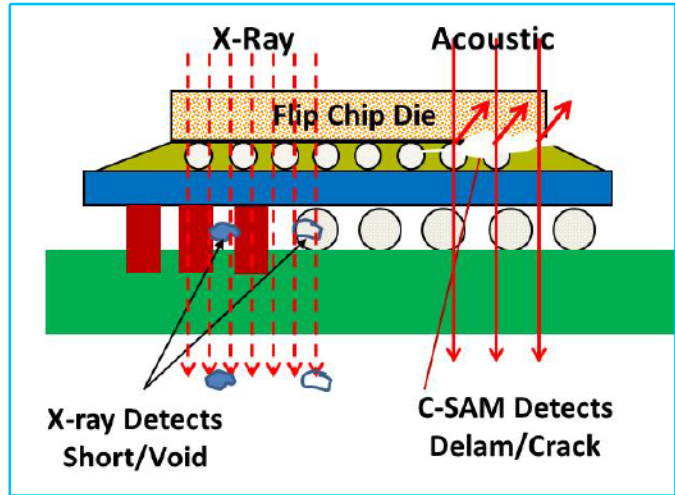


Figure 2-2. Key features of defect detectability by X-ray and C-SAM for flip-chip BGA/CGA.

At least three basic types of acoustic microscope have been developed. These are the scanning acoustic microscope (SAM), scanning laser acoustic microscope (SLAM), and C-mode scanning acoustic microscope (C-SAM). C-SAM uses the same transducer to pulse ultrasound and receive the return echoes, meaning that the acoustic image can easily be constrained to a depth of interest. It has the ability to create images by generating a pulse of ultrasound focused to a pinpoint spot. The pulse is sent into a sample and reflected off of interfaces (see Figure 2.3). The frequency of the pulse and design of the lens are chosen to optimize spot size resolution and depth penetration for each application. In the reflection mode of operation the same transducer is used to send and receive the ultrasonic pulse. Return echoes arrive at different times based upon the depth of the reflecting feature and the velocity of sound in the materials. The operator positions an electronic gate to capture the depth of interest. The amount of ultrasound reflected at the interface is based on the differences in the materials at the interface. The more different the materials the more ultrasound reflected.

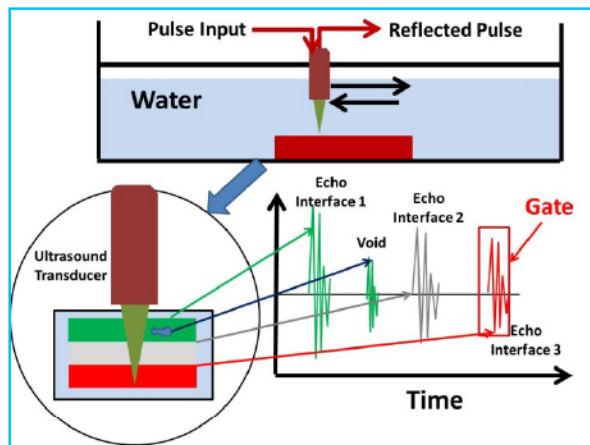
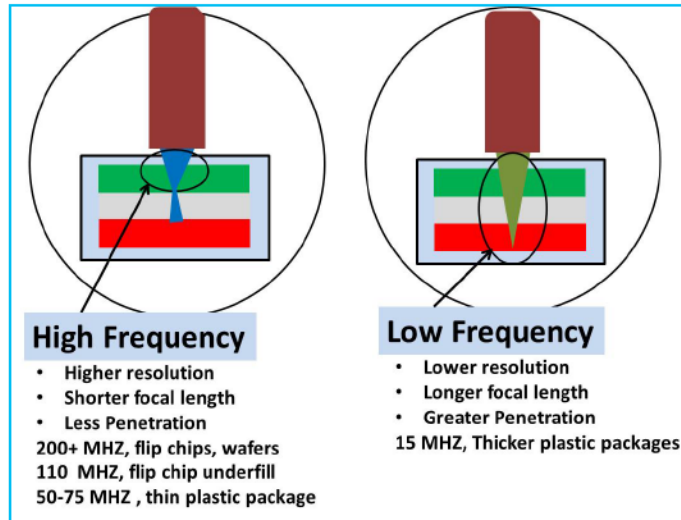


Figure 2-3. Key features of C-SAM operation and detection of defects including voids and delamination.

Similar to X-ray, acoustic microscopy is a non-destructive technique for visualization of defects, widely used in the production of electronic components and assemblies for quality control, reliability and failure analysis. Usually the interest is in finding and analyzing internal defects such as delaminations, cracks and voids, although an acoustic microscope may also be used simply to verify (by material characterization or imaging, or both) that a given part or a given material meets specifications or, in some instances, is not counterfeit. Acoustic microscopes are also used to image printed circuit boards and other assemblies.

The ultrasonic frequencies pulsed into samples by the transducers of acoustic microscopes range from a low of 10 MHz (rarely, 5 MHz) to a high of 400 MHz or more. Across this spectrum of frequencies there is a trade-off of penetration and resolution. Ultrasound at low frequencies (such as 10 MHz) penetrates deeper into materials than ultrasound at higher frequencies (see Figure 2.4), but the spatial resolution of the acoustic image is less. On the other hand, ultrasound at very high frequencies does not penetrate deeply, but provides acoustic images having very high resolution. The frequency chosen to image a particular sample will depend on the geometry of the part and on the types of materials.



**Figure 2-4.** Selection of appropriate transducers is key in optimizing penetration and resolution for the flip-chip BGA and CGA.

## 2.4 AMI for Plastic Encapsulated Microcircuits (PEM) Evaluation

In a previous comprehensive study [7], the C-SAM nondestructive technique was used to evaluate COTS PEMs using samples from different commercial vendors for detecting internal defects due to various environmental exposures. PEM failure modes reported in industry due to delamination are summarized as:

- Stress-induced passivation damage over the die surface
- Wire-bond degradation due to shear displacement
- Accelerated metal corrosion
- Die-attach adhesion
- Intermittent electrical signals at high temperature
- Popcorn cracking
- Die cracking
- Device latch-up

Figure 2-5 shows one of the most common failure modes (popcorning) as a result of delamination, moisture accumulation, and pressure release within a plastic package during the board assembly process. Delamination is dependent on package construction, package size, die size, lead design, number of leads, and environmental stresses, among other influences.

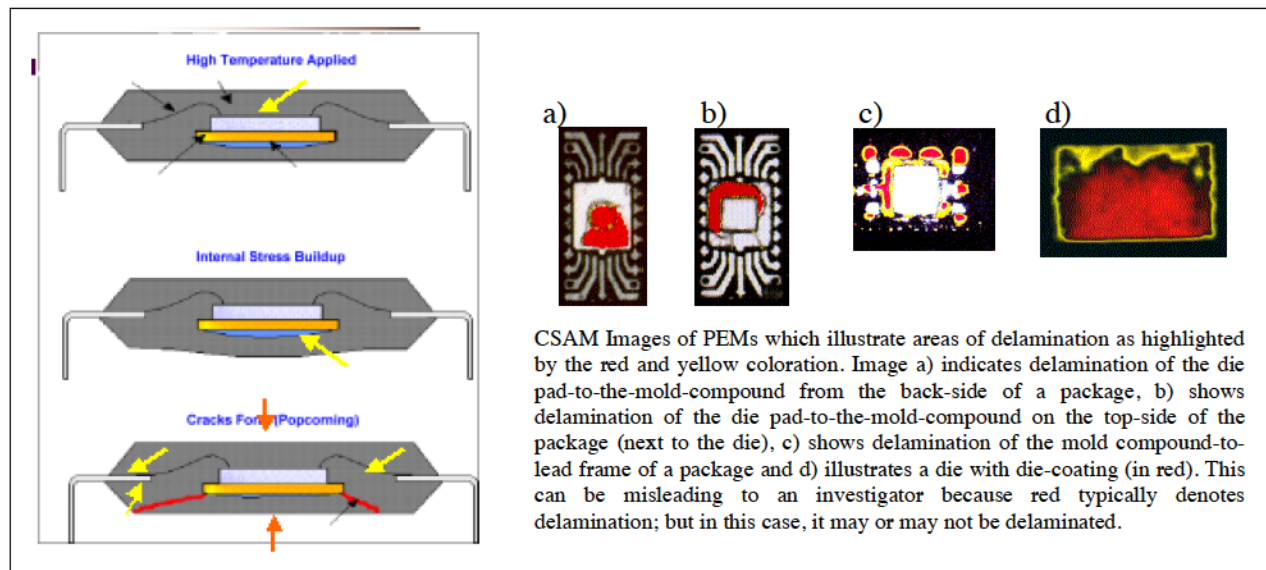


**Figure 2-5.** Examples of packages with delamination. The yellow arrows show areas where the existence of delamination can accelerate entry/collection of moisture; the red lines show where the cracks (popcoming) typically occur when the board is exposed to high temperature during assembly [7].

They reported a number of anomalies and potential reliability defects including delamination at die attach, at leads within the mold compound, around the die within the mold compound, on top of the die, and at the backside of the die paddle. The authors analyzed the defect anomalies by C-SAM imaging to determine their impact on the reliability of PEMs. C-SAM images from the beginning of a screening flow were used as a predictor of good or poor subsequent electrical performance of devices. Images tended to correlate with changes in electrical performance. C-SAM inspection and electrical parametric shifts of devices that were subjected to convection reflow were affected less than those equivalent devices exposed to hand soldering and vapor phase reflow (two zones, preheat and reflow).

In an investigation of defect detection for a multilayer ceramic capacitor (MLCC) [8], it was found that the 50-MHz transducer is more effective in detecting defects during screening by C-SAM than a 30-MHz version. Screening at a higher frequency enabled reducing rejection that was initially discovered during the board level testing. It saved costly rework at the board level even though there was a slight cost increase due to additional MLCC rejection.

## 2.5 C-SAM of Flip-Chip and Underfill

AMI has been used since early 2000 [9] with the introduction of ultra-high frequency transducers to analyze flip chip underfill and interconnect bonds. It was shown that defects such as delamination and void can be detected at each layer and, with 3V (virtual volumetric viewing), the 3D morphology and depth location of the defects can give important information as to the cause of the flaws (see Figure 2.6). Transducers and imaging techniques provided focused access of the ultrasound beam to the interface of interest (chip/ bump and underfill, or bump and underfill/substrate) through any thickness of silicon commonly encountered. The first application images illustrate some of the early work done to improve the resolution in the acoustic images for flip chips. The images compare the sample at 180 MHz to another sample using a 230-MHz transducer. There is a significant improvement in the resolution in the image using an adapted 230-MHz transducer to detect finer pitch flip-chip die and traces. The specific transducer was able to correct for the edge effects and improve resolution. The white features in the images correspond to underfill voids.

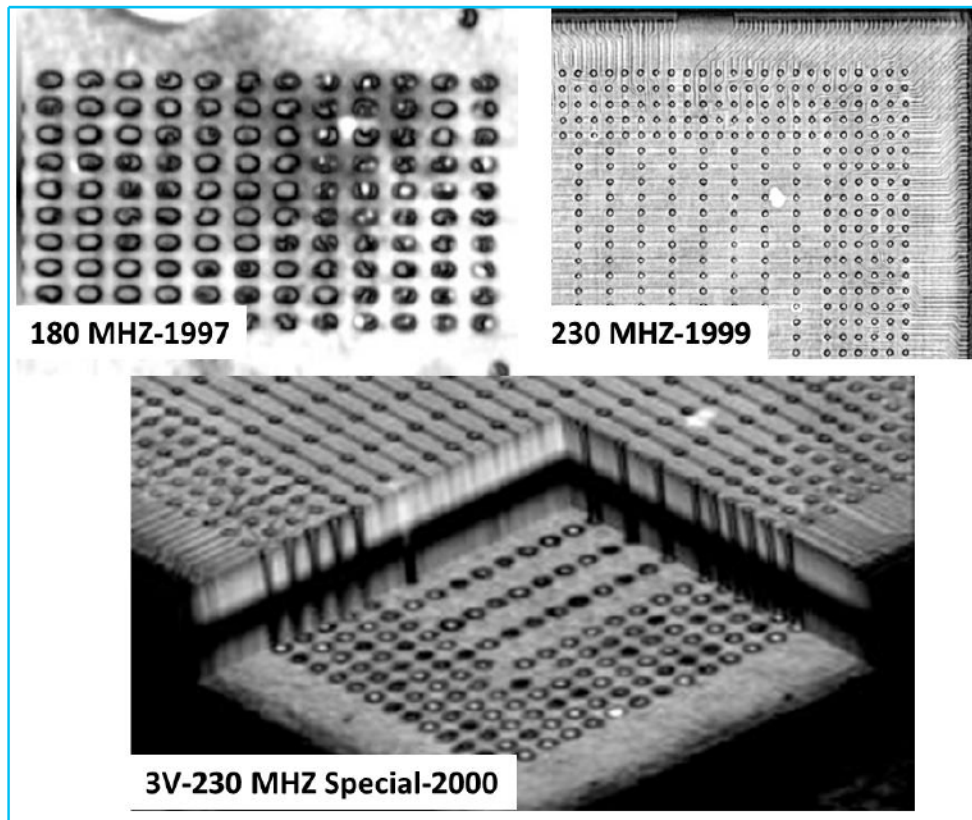


**Figure 2-6.** Improvement in resolution, as it relates to use of 3V (virtual volumetric viewing) to better define morphology and location of defects by C-SAM for flip-chip technology [8].

The interface scans are level-specific and several images are required to cover the entire volume of the device. This is usually not a major issue with regard to flip chips, as the pertinent information for evaluation of the underfill and bump quality is contained in the images of two interfaces. However, there are instances where additional information can be useful. The lower half of Figure 2.6 is a 3D image of the flip-chip C-SAM slices. By using 3V reconstruction a number of images or “slices” can automatically be taken covering the entire underfill thickness and reconstructed into an electronic model of the sample. The sample can then be repeatedly sectioned and reconstructed in order to fully analyze features and defects at any depth within the volume of the part. The challenge is still the interpretation of the information contained in the images, which relies on the capability of a trained investigator.

Two color acoustic images shown in Figure 2.7 clearly depict full or partial disband of solder balls and voids in the underfill in a flip-chip assembly [10]. The conditions were as follows:

- A flip-chip package (top image) was imaged from the top side from the back of the die at the high acoustic frequency of 230 MHz using a high resolution scan of 1024x960 pixels. Gating, region of set AE echo, was on the interface between the die face and the underfill material; therefore, the condition of bonding pads onto the die face was revealed. Red bumps are those where bonding is absent or is incomplete, the small red halo defects, near some bumps, are a vertical delamination in the underfill.
- A different flip-chip package (bottom image) was imaged from the bottom substrate side. Gating was on the interface between the cured underfill and the substrate; therefore bonding the solder balls to their pads. Red areas represent large voids in the underfill. The white areas are incomplete, indicating that these solder balls are only partially bonded.

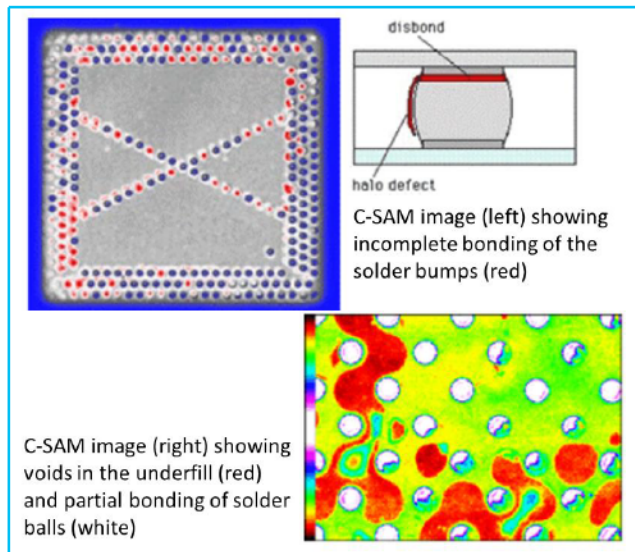


**Figure 2-7.** Defect detection by C-SAM for flip-chip technology (see reference [10]).

In the development of Pb-free flip-chip packaging of ultra-low k (ULK) technology of Si chips on organic substrate [11], the authors effectively first used non-destructive techniques to improve flip-chip assembly—and then it used destructive technique for verification of the improvements made. Both C-SAM and X-ray NDE images were presented (see Figure 2.8) for an assembly prior to its optimization by a differential heating/cooling chip joint method. The C-SAM investigation detected fractures in the ULK layers, whereas X-ray techniques identified solder joint bridging.

In a recent investigation [12], the author states that even though the 200 MHz transducer can detect gross defects, it does not have sufficient resolution to detect voids in a through silicon vias (TSV). Micron size defect detection required the development of a C-SAM transducer with 1 GHz capability. Such a high frequency transducer allowed good and bad TSVs to be distinguished in a number of test samples.

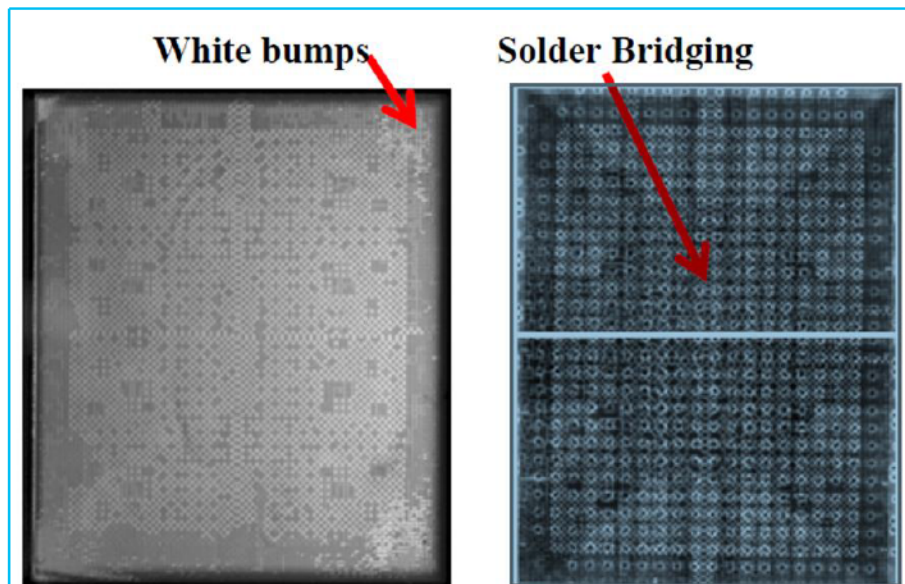


**Figure 2-8.** Types of defect detection by C-SAM (left) and X-ray (right) for flip-chip technology (see reference [11]).

## 3.0 EXPERIMENTAL EVALUATION BY C-SAM

### 3.1 Test Plan and Evaluation Approaches

This section covers evaluation performed by C-SAM using a number of advanced packages and assemblies before and after various environmental exposure. Representative flip-chip plastic and ceramic area array (ball/column) packages and assemblies from the previous investigations were subjected to C-SAM evaluation. It also included recently acquired land grid array packages and fine pitch assemblies. Key packages evaluated included are:

- A plastic land grid array after assembly. Because of extremely low stand-off, it was extremely difficult to visually inspect solder interconnections. It was thought that C-SAM technique may provides an insight into integrity of solder interconnections.
- A ceramic flip-chip LGA package with 1517 I/O, which were previously assembled onto PCB and then removed, was subjected to C-SAM evaluation. So, the flip-chip die was exposed to two reflow cycles. Since the flip-chip die had no heat sink attachment , its back was exposed. Also, a CGA assembly version of this LGA package, which were previously assembled onto PCB and subjected to thermal cycling, was included in the C-SAM evaluation.
- A flip-chip CGA1752 I/O package assembly was also subject to C-SAM evaluation. It was realized that this package has an extra heat sink attachment; therefore, the acoustic signal from bonding materials will be a dominant signal.
- A flip-chip BGA1704 I/O package assembly was also subjected to C-SAM evaluation. The flip-chip die of this package, similar to its ceramic CGA 1752 counterpart, also had an extra interface due to heat sink attachment. This package assembly previously was subjected to a number of thermal cycles.
- The FC-CGA 1752 I/O after its heat sink was removed was re-examined. This CGA was re-evaluated by C-SAM for integrity of the flip-chip solder joints since original package showed only integrity of heat sink bonding materials.
- A hermetically sealed CGA with 1272 columns, which had die wire bonded, was also subject to C-SAM evaluation to determine if internal integrity of wire bonds could be assessed.
- A large number of fine pitch and stack package assemblies were subjected to C-SAM to evaluate their integrity and appropriateness of C-SAM.
- The FC-CGA 1752 package with no heat sink along with a fine pitch package was subjected to cycles up to 20 times of solder iron touch to induce defects. These were re-scanned to determine the level of damage and their detectability by the C-SAM technique.
- Cross-sectional examinations were performed for the LGA 1517 I/O to correlate the C-SAM images with optical microscopy images.

To achieve the highest results with limited funding, this investigation examined only packages as individual or test vehicles built previously, either used as is or subjected to thermal cycling conditions. Ideally, new test vehicles with inducing known defects should add additional values and will be pursued if additional funds become available. The purpose of using such a mix of packages and assemblies was to initially determine the benefits of C-SAM and to determine its potential limitations, especially FCBGA and FC-CGA. Detailed information on package including internal configuration, optical photomicrographs, X-ray and as well C-SAM images using a range of transducers are also presented. Both outside facilities with extensive equipment capability and an experienced operator, as well as internal C-SAM equipment with a lower capability and less experienced operator, were considered in this evaluation. Results are presented.

### 3.2 Plastic LGA132

Figure 3.1 compares an optical photomicrograph image of a plastic LGA package assembly with 132 lands and their X-ray and C-SAM images. The C-SAM image was taken using a very low frequency transducer of 5 MHz in order enable deeper acoustic wave penetration into the package for comparison to its X-ray images. The C-SAM image shows a few key internal chips similar to X-ray, but several other details are missing. The X-ray shows greater detail of internal package configuration, including solder on land pads and land shape (e.g., a square land on the top left). Layering image is impossible with the 2D X-ray, but it can be performed by the C-

SAM technique. Figure 3.2 shows C-SAM layering images using a 25 MHz transducer. It clearly shows different interfaces in package assembly from the top to the bottom.

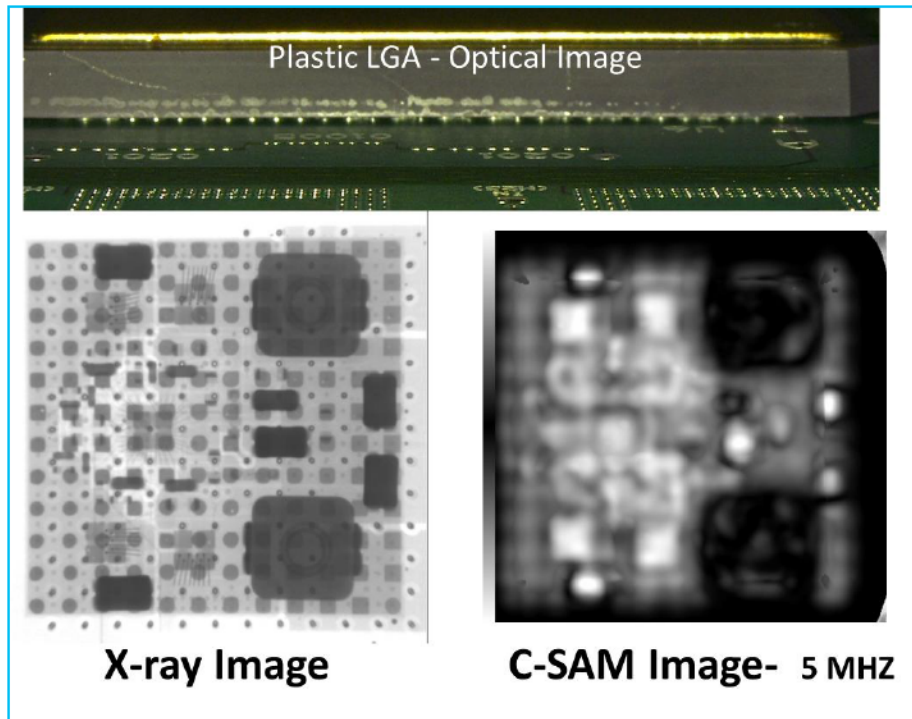


Figure 3-1. Comparison images by optical microscopy (top), by X-ray (bottom left) and by C-SAM from the LGA 132 I/O assembly.

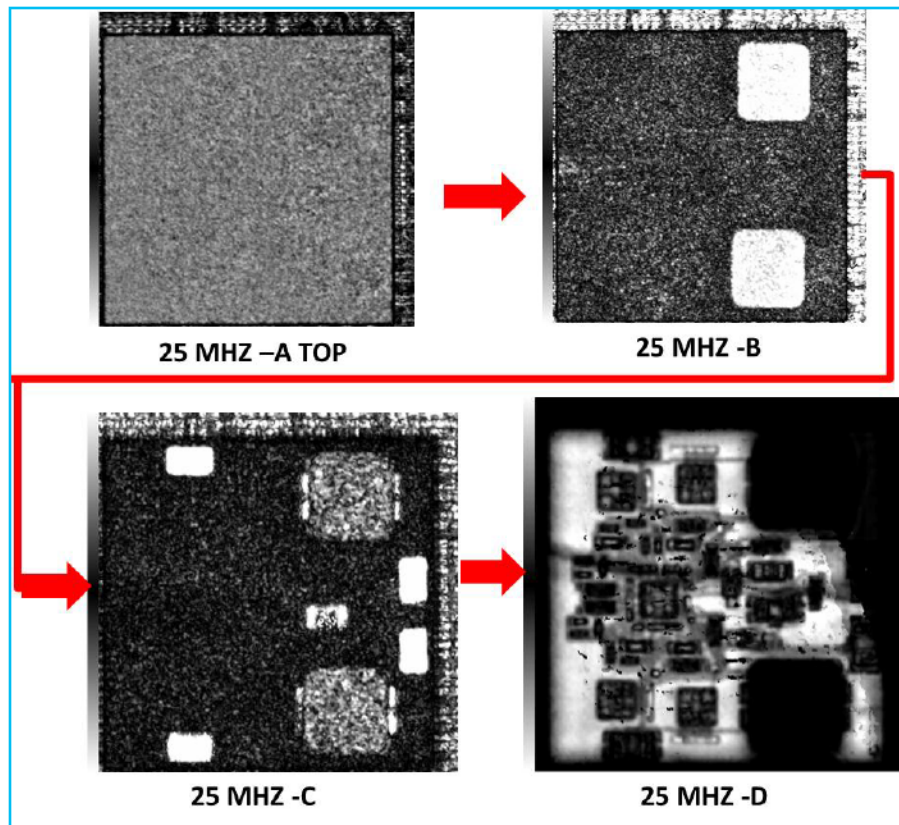
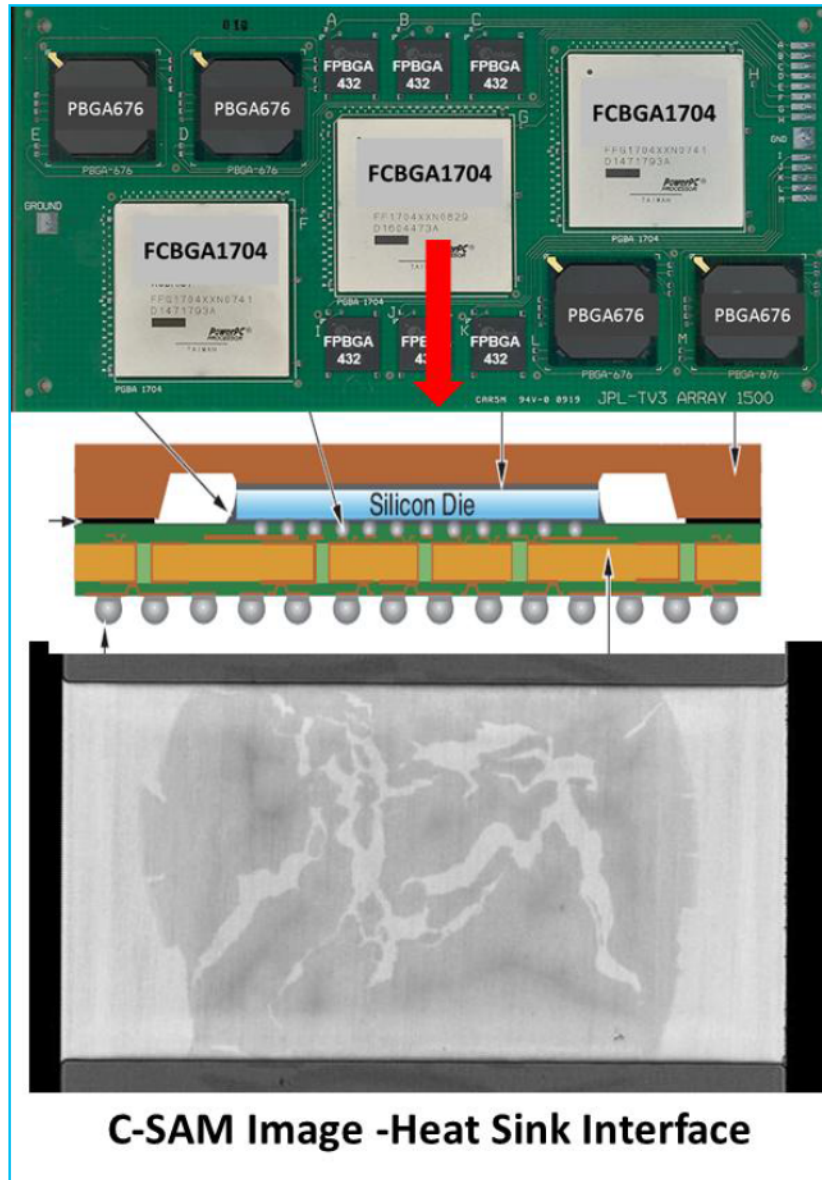


Figure 3-2. C-SAM layering images taken from the top to the internal LGA package assembly.

### 3.3 Flip-Chip BGA1704 with Heat Sink

The cross-sectional photomicrograph from a FCBGA1704, which was previously subjected to a number of thermal cycles, is shown in Figure 3.3. It is apparent that the back of the flip-chip die is covered by a heat sink that extended over the edge of the die, covering the flip-chip area. The only feature that could be revealed through C-SAM evaluation was the bonding condition of the thermal interface material (TIM). No information regarding underfill or solder bump condition below the TIM could be revealed due to this interface interference with the layers of interest. Hence, the heat sink hindered C-SAM evaluation.



**Figure 3-3.** C-SAM image for plastic FC-BGA 1704 I/O assembly showing the heat sink interface, which hindered further penetration of singals.

### 3.4 Flip-Chip CGA1752 with Heat Sink

The schematic drawing of FC-CGA1752 is illustrated in Figure 3.4. It is apparent that this package has an additional heat sink that overshadows the flip-chip die, explaining the C-SAM signal interference with the TIM interface. Due to the TIM inteferece, no layering imaging was possible. The heat sink restricted the C-SAM evaluation.

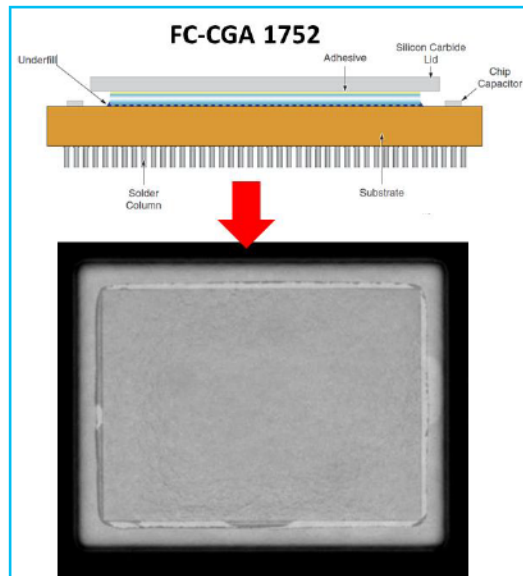


Figure 3-4. C-SAM image for FC-CGA 1752 I/O assembly showing heat sink interface, which hinders further penetration of singals.

### 3.5 Flip-Chip LGA1517/CGA without Heat Sink

This ceramic LGA package was ideal for revealing the integrity of the flip-die, since its heat sink was yet to be attached. Two styles of LGAs with 1517 I/Os were evaluated; one as a package and the other as an assembly. Irrespective of the package being alone or in an assembly, there was no heat sink and the back of the flip-chip die was exposed. There was no C-SAM signal interference due to the TIM as it was the case for CGA 1752 I/O. The first interface was between the die and solder bump and underfill. The second was between substrate and the land pads or solder joints of columns. Figures 3.5 to 3.7 show three C-SAM images taken with three different transducers with increasing frequencies of 25-, 100-, and 230-MHz. It is apparent that as frequency increases the granularity of the C-SAM image increases due to increase in spatial resolution. The details of the flip-chip solder bumps became apparent at a higher frequency. There is a dark region, which is surrounding the central white region. The dark area is postulated to be a total separation of underfill, but needs to be verified. A similar separation condition was also observed for the other LGA 1517 I/O package assembly (SN041), as shown Figure 3.8

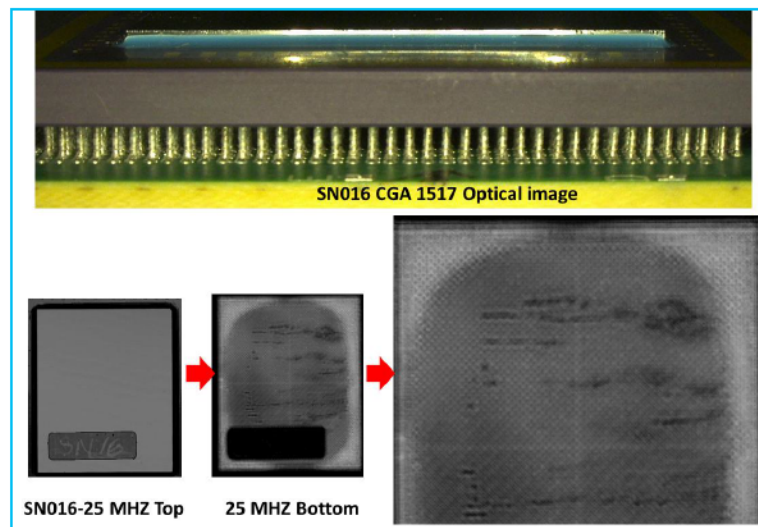


Figure 3-5. Optical and C-SAM ( at 25 MHz) layering images for FC-CGA 1517 assembly (SN016) showing flip-chip top and flip chip bump interface. This package had no heat sink.

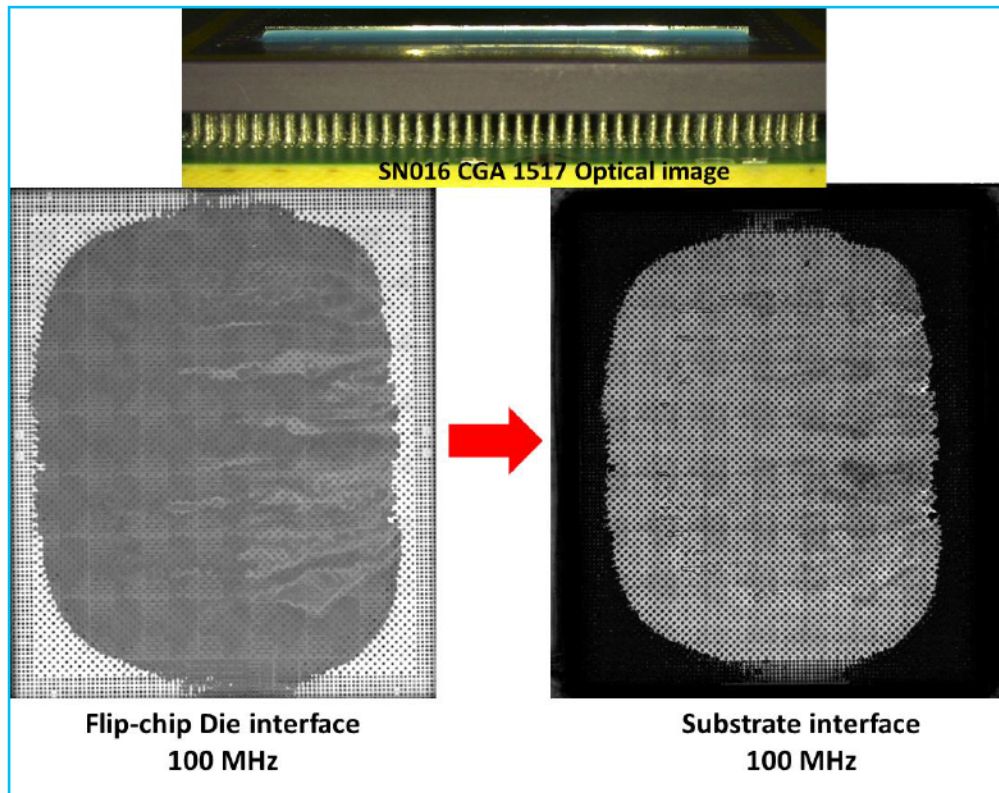


Figure 3-6. Optical and C-SAM ( at 100 MHz) images for FC-CGA 1517 assembly (SN016) showing images for die and substrate interfaces.

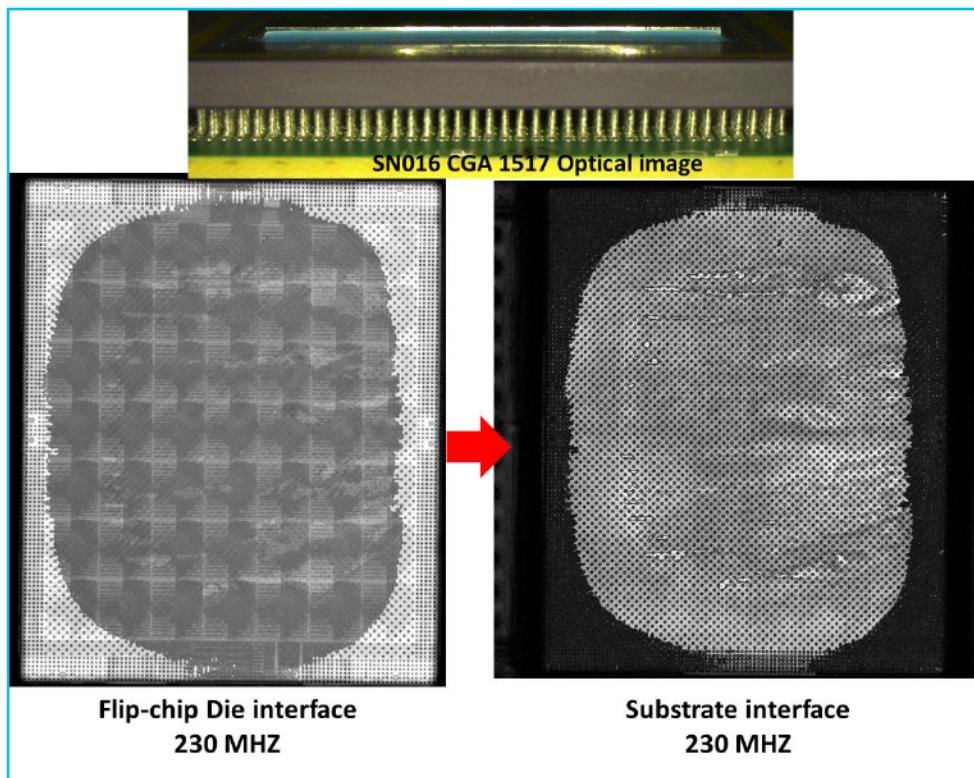


Figure 3-7. Optical and C-SAM ( at 230 MHz) images for FC-CGA 1517 assembly (SN016) showing images for die and substrate interfaces.

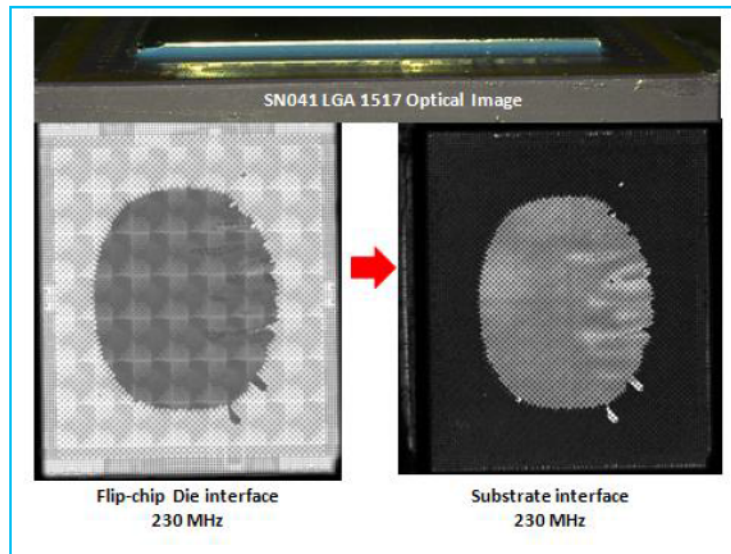


Figure 3-8. Optical and C-SAM ( at 230 MHz) images for FC-CGA 1517 assembly (SN041) showing images for die and substrate interfaces.

### 3.6 Fine Pitch PBGAs 432 and 676 I/O

Two plastic ball grid array package assemblies, one with 432 balls and 0.4-mm pitch and the other with 676 balls and 1-mm pitch, were subjected to C-SAM evaluation. Figure 3.9 shows the C-SAM images for these packages as well an optical picture of the test vehicle and the package assemblies. Generally, the C-SAM method is recommended for inspection of individual packages before assembly. Prevalent delamination and “popcorn” cracking in PBGA can be detected. Nevertheless, a few features of packages such as die configuration and outline, as well as attachment condition with no signs of popcorn delamination, could be identified. However, the integrity of solder ball attachment and solder joints on the board are unidentifiable. Multiple interfaces hinders accurate C-SAM evaluation of hidden solders under the package.

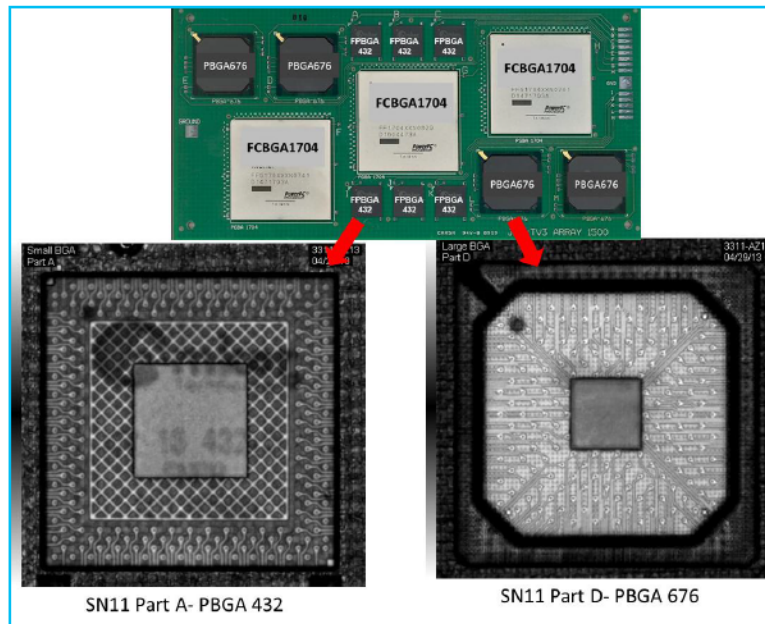


Figure 3-9. Optical and C-SAM images for fine pitch PBGA 432 I/O and PBGA 676 I/O.

### 3.7 C-SAM Repeat of CGA1752 after Heat Sink Removal

The initial C-SAM evaluation of FC-CGA 1752 I/O did not reveal the condition of the flip-chip die and underfill due to the package having a heat-sink interface. We successfully disbonded the heat from the die using a lap shear testing approach. The section of the flip-chip die with no heat sink was subjected to C-SAM evaluation to determine the condition of the flip-chip die and underfill. Figure 3.10 shows one optical and two C-SAM images of the CGA package. The condition of the flip-chip solder balls and joints appears to be acceptable. Only a small anomaly was detected in the underfill at the center of flip-chip die, as indicated by the arrow. To induce additional defects, this flip-chip CGA with no heat sink was subjected to 20 solder iron touches with a tip temperature of 700°F, each for about 5 seconds. No additional defects were detected. Other means need to be developed to induce controlled defects and evaluation by C-SAM.

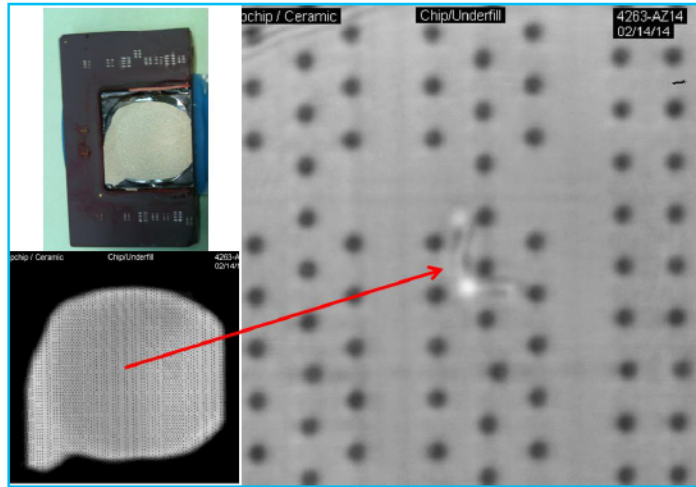


Figure 3-10. Optical (top left) and C-SAM images for FC-CGA 1752 I/O assembly after removal of the heat sink, showing the integrity of the flip-chip assembly and minor defect anomaly.

### 3.8 Hermetically Sealed CGA1272 with Internal Wire Bonds

Figure 3-11 shows a C-SAM image of a CGA1272 I/O package assembly. Only outer surfaces including the lid brazing section could be detected by C-SAM.

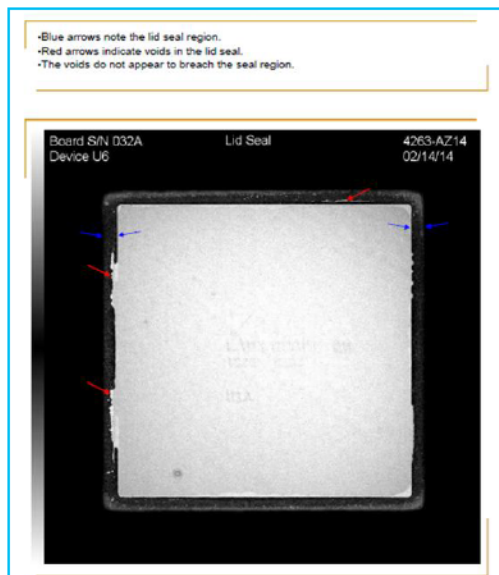


Figure 3-11. C-SAM images for a hermetically sealed CGA 1272 I/O assembly showing heat sink seal integrity. Blue arrows shows the lid seal region and red arrows show areas with voids.

### 3.9 Plastic LGA 1156 I/O and Fine Pitch Package Assemblies

Plastic LGA with 1156 I/O were subjected to C-SAM evaluation. Figure 3.12 shows images of this package. No defect anomaly was detected by C-SAM. Characterization was limited to the top section only. A number of other fine pitch plastic packages were also imaged. No defect anomaly was detected.

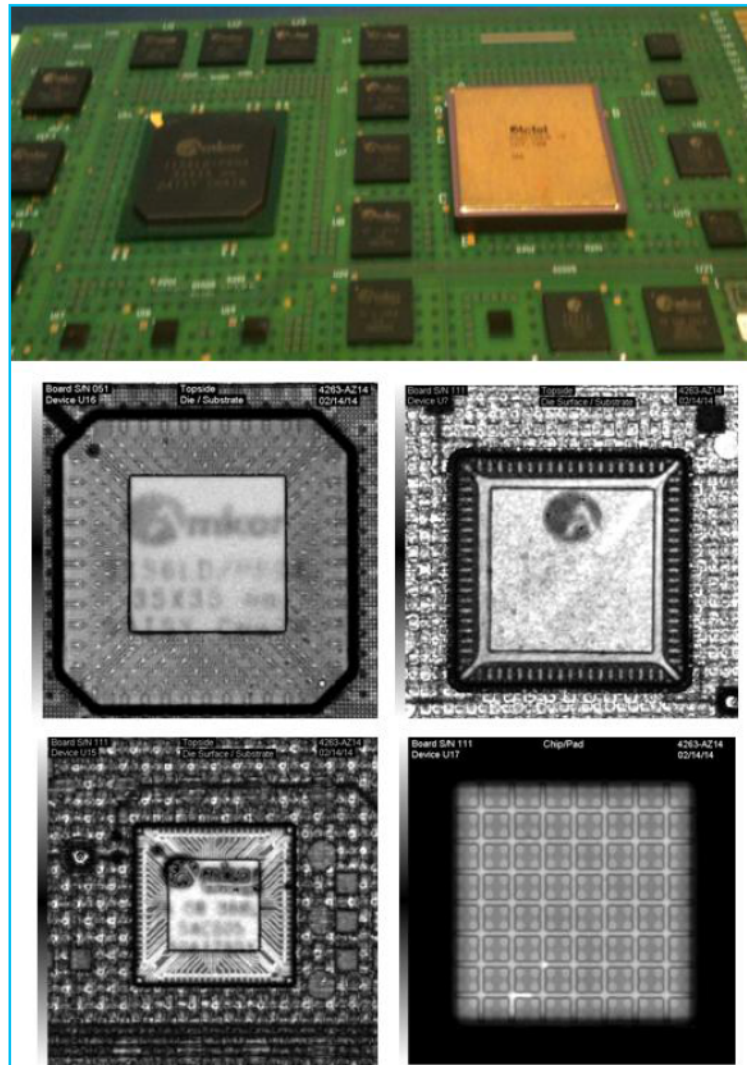
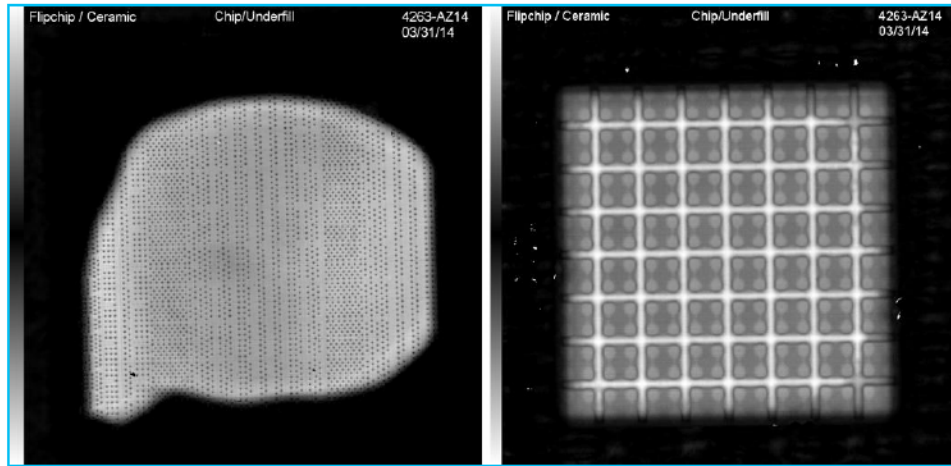


Figure 3-12. Optical (top) and representative C-SAM images for various PBGA and FPGA package assemblies.

### 3.10 Effect of 20 Solder Iron Touches at 700°F

CGA 1752 I/O without heat sink and one fine pitch plastic BGA package assembly was subjected up to 20 solder iron touches at 700°F, each for about 5 seconds. C-SAM was performed at 5, 10, and 20 exposures. Figure 3.13 shows C-SAM images after twenty touch ups. No anomaly was detectable for either package after 20 touches.



**Figure 3-13.** C-SAM images for FC-CGA 1752 I/O and FPBGA after 20 touches with a solder iron with 700F tip temperature. No apparent changes were revealed.

### 3.11 Cross-sectional Characterization of LGA1517

The flip-chip ceramic LGA1517 package was cross-sectioned to verify the condition of solder bump solder joints and underfill integrity. This package was selected for X-sectioning since it clearly showed a large dark area on the periphery of the die with minor shadowing at the center of the die. Figure 3.14 shows the optical image of X-sectioned LGA package at lower and higher magnifications. Inspection of the X-sectioned samples did not reveal any separation in the periphery of the die, as revealed by the C-SAM images. The reason for this discrepancy is unknown.

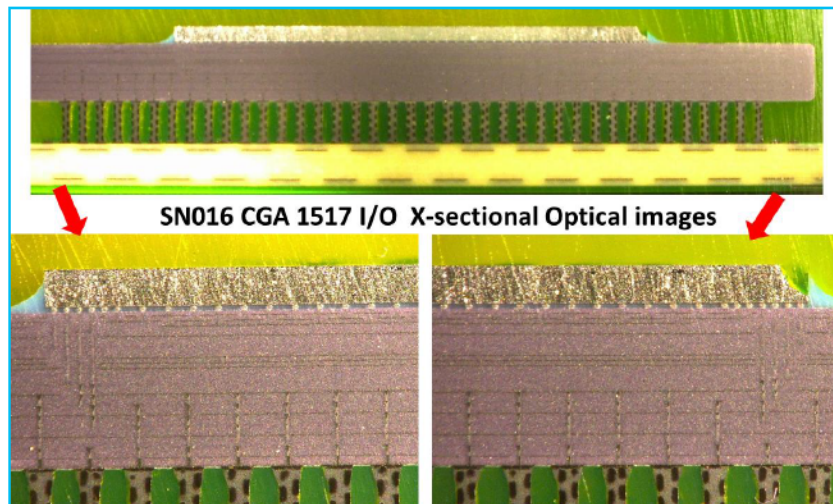


**Figure 3-14.** Optical image of a microsection of FC-CGA 1517 assembly (SN016), showing images for die and underfill.

## 4.0 CONCLUSIONS

The evaluations covered in this report deal with inspection methods and comparison of inspection results performed for advanced flip-chip column grid array, flip-chip ball grid, and a number of other fine pitch ball grid array and land grid array package assemblies. Visual inspection using optical microscopy has been the traditional approach for acceptance/rejection of workmanship defects by quality assurance personnel. Inspection of hidden elements in FC-CGA and FCBGA package assemblies requires using nondestructive inspection tools such as 2D/3D X-ray and, potentially, acoustic microscopic imaging. Limitations on using acoustic emission for solder joint assemblies are yet to be fully established.

AE and X-ray are complementary techniques that are frequently found in the same laboratories, but they reveal different features. X-ray detects features based on differential attenuation of the X-ray energy, whereas AE detects features based on materials changes. The practical result is that AE is orders of magnitude more sensitive for detecting air-gap defects such as voids, delaminations and cracks. C-mode scanning acoustic microscopy was evaluated for advanced electronic packaging assemblies, particularly FC-CGA and FCBGA. Inspection evaluations revealed the following results.

- Visual inspection by optical microscopy is ideal for detecting exposed features such as dewetting, microcracks, cold, and disturbed solder joint.
- Visual inspection is possible for periphery columns in CGA and balls in BGA, but is difficult for joints in a plastic land grid array due to a lower gap height. A 2D X-ray revealed many internal features of the LGA package including chips and solder joints.
- Layering C-SAM using a low frequency transducer revealed many features of the plastic LGA package assembly detected by X-ray; however, the features were less clear and it did not reveal package and board interfaces or solder joint conditions.
- It was revealed that C-SAM could only show the quality of heat-sink thermal interface bonding materials of the FC-CGA 1752 I/O. Heat sink is part of the package and is attached with adhesive on top of the flip-chip die, hence, it hindered penetration by acoustic emission signal into bumps and adhesive interfaces.
- C-SAM revealed the flip-chip bumps and underfill conditions of the FC-CGA package after shearing off its heat sink.
- The C-SAM revealed an edge delamination for FC-CGA 1517 I/O assembly since it had no heat sink on the flip-chip die. This allowed C-SAM characterization of the flip-chip bumps and underfill materials.
- Microscopic cross-sectional evaluation of FC-CGA 1517 did not support the edge-delamination revealed by the C-SAM images.
- C-SAM of a hermetically sealed LGA 1272 package revealed only the lid bonding defects. Internal features could not be detected. For plastic LGA1156, the C-SAM revealed only the die, but not the solder joint condition.
- C-SAM of a large number of other fine pitch ball grid array assemblies revealed internal die integrity and configuration, but it did not show solder ball or joint attachment integrity.
- No defect was detected by C-SAM when CGA 1752 I/O and fine pitch BGA packages with 20 repeated solder iron touches, each for about 5 seconds using a tip temperature of 700°F.

Non-destructive evaluation of microelectronic packaging and assemblies is of critical importance in assuring reliability. Understanding key features of various NDE inspection systems in detecting defects in the early stages of assembly are critical to developing approaches that will minimize future failures. Additional specific, tailored, NDE inspection approaches could enable low-risk insertion of these advanced electronic packages.

Even though C-SAM showed significantly lower versatility in defect detection compared to X-ray for packages and assemblies of FC-CGA and FCBGA, the C-SAM techniques are widely used for detection of flip-chip die attachment by package manufacturers during the early stages of the flip-chip die assembly. However, added additional interfaces, e.g. heat sink on die, limits the use of acoustic emission approach at package and assembly levels.

C-SAM inspection is a non-destructive technique with a wider use for revealing hidden gap defects, including delamination and voids. It is recommended that the C-SAM characterization be used as a complement to other inspection techniques, including X-ray and traditional visual inspection by optical microscopy. It is apparent that

a combination of various inspection techniques may be required in order to assure quality at part, package, and system levels. This is especially true for newly introduced miniaturized advanced electronic packages with hidden flip-chip solder bumps at the die level and solder balls at the package level with associated underfill and solder joints.

## 5.0 REFERENCES

- [1] Ghaffarian, R., "Damage and Failures of CGA/BGA Assemblies under TC and Dynamic Loading," ASME, IMEC, San Diego, CA, Nov. 2013
- [2] Ghaffarian, R., "Thermal Cycle and Vibration/Drop Reliability of Area Array Package Assemblies," *Structural Dynamics of Electronics and Photonic Systems*, eds. E. Suhir, E. Connally, and D. Steinberg, Chapter 22, John Wiley, New York, NY, 2011.
- [3] Ghaffarian, R., "Thermal Cycle Reliability and Failure Mechanisms of CCGA and PBGA Assemblies with and without Corner Staking," *IEEE Transactions on Components and Packaging Technologies*, Vol. 31, Issue 2, 2008.
- [4] Ghaffarian, R. "CCGA Packages for Space Applications," *Microelectronics Reliability* **46** 2006–2024, 2006.
- [5] Fjelstad, J., Ghaffarian, R., and Kim, Y.G., *Chip Scale Packaging for Modern Electronics*, Electrochemical Publications, 2002.
- [6] <http://www.sonoscan.com/technology/ami-basics1-3.html>, Accessed Jan 27, 2014
- [7] Sandor, M., Agarwal, S., "Using Nondestructive Methods (C-SAM) for COTS PEMs Screening and Qualification," CMSE, Feb. 2001, <http://trs-new.jpl.nasa.gov/dspace/bitstream/2014/39431/1/01-0006.pdf>, Accessed Jan. 27, 2014
- [8] Kostic, A.D., Schwartz, S.W., "Optimized Acoustic Microscopy Screening for Multilayer Ceramic Capacitors," Proceedings of Reliability and Maintainability Symposium (RAM), 2011, Pages :1-4
- [9] Semmens, J. "Flip Chips and Acoustic Micro Imaging: An Overview of Past Applications, Present Status, And Roadmap for the Future," <http://www.sonoscan.com>, Accessed Jan 27, 2014
- [10] Kessler, L.W., " Probing Flip-Chip Interfaces," Mar. 1, 2006, <http://www.edn.com/design/test-and-measurement/4381152/Probing-flip-chip-interfaces>, Accessed Jan 27, 2014
- [11] Sakuma, K., Smith, K., Tunga, K., Perecto, E., Wassick, T., Pompeo, F., Nah, J., "Differential Heating/Cooling Chip Joining Method to Prevent Package Interaction Issue in Large Die With Ultra Low-K Technology," Electronic Components and Technology Conference (ECTC), 2012
- [12] Phommahaxay, A., et al, "High Frequency Scanning Acoustic Microscopy Applied to 3D Integrated Process: Void Detection in Through Silicon Vias," Electronic Components and Technology Conference (ECTC), 2013

## 6.0 ACRONYMS AND ABBREVIATIONS

2D	two-dimension
3D	three-dimension
3V	virtual volumetric viewing
AE	acoustic emission
AMI	acoustic microimaging
BGA	ball grid array
CBGA	ceramic ball grid array
CCGA	ceramic column grid array
CGA	column grid array
COTS	commercial-off-the-shelf
CQFP	ceramic quad flat pack
C-SAM	C-mode scanning acoustic microscopy
ESD	electrostatic discharge
FC	flip chip
FCBGA	flip-chip ball grid array
FC-CGA	flip-chip column grid array
I/O	input/output
JPL	Jet Propulsion Laboratory
LGA	land grid array
MIP	mandatory inspection point
MLCC	multilayer ceramic capacitor
NASA	National Aeronautics and Space Administration
NDE	non destructive evaluation
NEPP	NASA Electronic Parts and Packaging
PBGA	plastic ball grid array
PCB	printed circuit board
PEM	plastic encapsulated microcircuit
PWB	printed wiring board
QA	quality assurance
ROHS	restriction on hazardous substances
SAM	scanning acoustic microscope
SLAM	scanning laser acoustic microscope
TIM	thermal interface material
TSV	through silicon via
ULK	ultra low-K
X-section	cross-section